

zation of these MO's permits only a fraction of the pair of electrons shown in these orbitals in Figure 2 to reside on the axial oxygen. Because of the negative charge on the terminal oxygens, the orbitals on these atoms may be expected to lie at higher energy than those on the ring oxygens. The energy level diagram in Figure 2b reflects the rise in energy of the axial oxygen lone-pair orbital as a result of the ring oxygen lone-pair interaction. The lower ionization potentials of the axial oxygen lone pairs could then account for the greater polarizability of this site by cations and alkylating nucleophiles.

Acknowledgment. J.G.V. thanks the National Cancer Institute of the National Institutes of Health for grant support of this research. The authors also thank one of the referees for

bringing to their attention the relevance of enolate alkylations to the present work.

References and Notes

- (1) J. G. Verkade, Plenary Lecture, 5th International Conference on Organic Phosphorus Chemistry, Gdansk, 1975; *Phosphorus*, in press, and references cited therein.
- (2) J. G. Verkade, *Bioinorg. Chem.*, **3**, 165 (1974).
- (3) R. F. Hudson and J. G. Verkade, *Tetrahedron Lett.*, 3231 (1975).
- (4) R. S. Edmundson, *Tetrahedron*, **21**, 2379 (1965).
- (5) D. W. White, R. D. Bertrand, G. K. McEwen, and J. G. Verkade, *J. Am. Chem. Soc.*, **92**, 7125 (1970).
- (6) D. M. G. Martin, C. B. Reese, and G. F. Stephenson, *Biochemistry*, **7**, 1406 (1968).
- (7) "Organic Synthesis", Collect. Vol. 2, Wiley, New York, N.Y., 1943, p 462.
- (8) J. A. Mosbo and J. G. Verkade, *J. Am. Chem. Soc.*, **95**, 4659 (1973).
- (9) H. O. House, "Modern Synthetic Reactions", W. A. Benjamin, Inc., Menlo Park, Calif., 1972, Chapter 9, and references cited therein.
- (10) J. Engels and W. Pfeleiderer, *Tetrahedron Lett.*, 1661 (1975).

High-Resolution Boron-11 Nuclear Magnetic Resonance Spectroscopy. 6. ¹ Application of Relaxation Time Measurements to Boron Hydrides

Edward J. Stampf,² Albert R. Garber, Jerome D. Odom,* and Paul D. Ellis*

Contribution from the Department of Chemistry, University of South Carolina, Columbia, South Carolina 29208. Received February 10, 1976

Abstract: The spin-lattice and transverse relaxation times of small boron hydrides and several derivatives are reported. Measurement of T_1 and T_2 relaxation rates of magnetically dilute boron-10 in several compounds confirms that the quadrupolar mechanism dominates transverse as well as spin-lattice relaxation in small boron hydrides. Assured that $T_1 = T_2$, unresolved boron-boron coupling constants are estimated by line shape analyses employing measured T_1 relaxation rates. The magnitude of J_{BB} is related to the bonding between the coupled nuclei and a correlation of observed boron-boron coupling constants with current localized molecular orbital views of boron hydrides is demonstrated.

In earlier papers of this series, we have reported several factors that influence the magnitude of the boron-boron coupling constant, J_{BB} .³ Of particular interest here is the dependence of the magnitude of J_{BB} on the bonding situation between the coupled atoms. For example, a rather large coupling constant of 19.4 Hz between the apex and basal borons in B_5H_9 has been reported.⁴ In contrast, a reasonable upper limit for J_{BB} transmitted through a bridge hydrogen has been reported to be 1.1 Hz for B_2H_6 and 0.3 Hz for B_4H_{10} .⁵ Prompted by this significant variance in the magnitude of J_{BB} for the two different bonding environments already investigated, we undertook this study to further investigate the value of J_{BB} for other common bonding situations, i.e., for boron atoms coupled through a pure three-center, two-electron bond or through a two-center, two-electron bond.

Several techniques have been established that were necessary for the determination of these coupling constants. Utilization of triple resonance techniques⁵ and complete proton decoupling⁴ met with limited success. For resonances in which J_{BB} approaches the natural line width, a poorly resolved multiplet or broad single line results. Line narrowing techniques⁶ can overcome this problem to an extent and have made it possible to abstract additional coupling constants.⁷ However, this method has a lower limit of resolution of approximately 10 Hz in this application.

In this paper we describe another technique which has allowed us to estimate coupling constants which were previously inaccessible by other methods. This technique involves mea-

surement of spin-lattice relaxation times (T_1) and utilization of the T_1 data in an FT NMR line simulation program.⁸

For a Lorentzian line, the half-height line width ($\Delta\nu_{1/2}$) is defined as $1/\pi T_2^*$, where $1/T_2^* = 1/T_2 + (\gamma\Delta H_0/2)$. Thus the observed line width, in the absence of any coupling, contains contributions from the transverse relaxation time (T_2) and inhomogeneity in the magnetic field (ΔH_0).

For the ¹¹B nucleus, previous studies⁹ have shown that the quadrupolar mechanism dominates spin-lattice relaxation and that all other mechanisms contribute negligibly. If the extreme narrowing condition¹⁰ ($\omega_0^2\tau_c^2 \ll 1$) is valid, it has been generally assumed that $T_1 = T_2$. Implicit in this assumption is the requirement that no other mechanism (e.g., scalar coupling) contributes to transverse relaxation. This assumption is further investigated and shown to be valid.

We have measured the spin-lattice relaxation times of several boron hydrides and derivatives. Utilizing these data, we have abstracted J_{BB} by fitting the calculated spectrum to the experimental line shape. Since the observed resonance line shape contains a contribution from inhomogeneity in H_0 , the coupling constants so derived represent an upper limit to J_{BB} . Qualitatively, we have found that there is a correlation between the magnitude of J_{BB} and the nature of the bond between the coupled nuclei.

Experimental Section

Standard high-vacuum techniques were used throughout this study.¹¹ The purity of all compounds was checked by vapor pressure

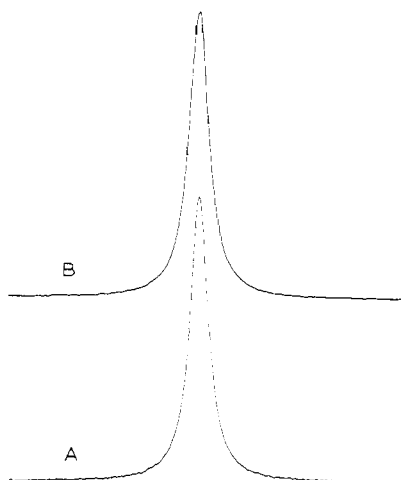


Figure 1. Calculated and observed 32.1-MHz ^{11}B NMR spectra of $^{11}\text{B}_2\text{H}_6$: (A) simulated line shape utilizing the experimentally determined T_1 of 24.2 ms and $J_{\text{BB}} = 0.0$ Hz; (B) the observed spectrum, $\Delta\nu_{1/2} = 14.0$ Hz.

measurement, ir, and/or ^{11}B NMR spectroscopy. Isotopically enriched $^{11}\text{B}_2\text{H}_6$ was prepared by lithium aluminum hydride reduction of 96.8% $^{11}\text{BF}_3\cdot\text{O}(\text{CH}_3)_2$ (Oak Ridge National Laboratory).¹² Enriched $^{11}\text{B}_4\text{H}_{10}$ was prepared by the gas-phase pyrolysis of $^{11}\text{B}_2\text{H}_6$ in a circulatory system equipped with a hot zone of 135 °C and a cold trap maintained at approximately -120 °C. Triborane(7)-carbonyl and tetraborane(8)-carbonyl were prepared according to published procedures.^{13,14} The bases, HPF_2 and $(\text{CH}_3)_2\text{NPF}_2$, were also prepared according to literature preparations;^{15,16} PF_3 was obtained commercially (Ozark-Mahoning Co.). The compounds $\text{B}_4\text{H}_8\cdot\text{L}$ (L = PF_3 , $(\text{CH}_3)_2\text{NPF}_2$, HPF_2) were all prepared from $\text{B}_4\text{H}_8\cdot\text{CO}$ through displacement of CO by the appropriate base.^{17,18} The reaction vessel was periodically frozen to -196 °C and CO pumped away via a Toepler pump until no further CO was generated. Yields of 84.0, 66.4, and 79.7% were obtained for $\text{B}_4\text{H}_8\cdot\text{PF}_3$, $\text{B}_4\text{H}_8\cdot\text{HPF}_2$, and $\text{B}_4\text{H}_8\cdot\text{PF}_2\text{N}(\text{CH}_3)_2$, respectively, based on the starting quantity of $\text{B}_4\text{H}_8\cdot\text{CO}$. The compounds $\text{B}(\text{OCH}_3)_3$, B_5H_9 , B_5H_{11} , and $\text{B}_{10}\text{H}_{14}$ were obtained from available laboratory supplies.

The Fourier transform NMR spectra were obtained on a Varian Associates XL-100-15 spectrometer operating in the GyroCode Observe mode (^{10}B , 10.7 MHz; ^{11}B , 32.1 MHz). All samples were run as 20% solutions in C_7D_8 , except where otherwise stated. Standard variable temperature equipment was used. Temperatures were checked before and after each T_1 experiment and were consistent to ± 0.5 °C. The T_1 's were measured under conditions of complete ^1H decoupling using the Freeman-Hill pulse sequence $(-T-90^\circ-T-180^\circ-\tau-90^\circ)-\text{N}$, where the recycle time T was chosen to exceed five times the longest T_1 to be measured. At least 100 transients were accumulated for each τ and a minimum of ten τ values were used in the standard least-squares analysis. The reproducibility of the T_1 's from experiments run on different days was better than $\pm 5\%$. The T_2 's were measured by the Carr-Purcell-Meiboom-Gill¹⁹ pulse sequence $90^\circ_x-(\tau-180^\circ_y-\tau)-\text{N}$ AT, where $\tau = 1$ ms and the last half echo is accumulated and Fourier transformed.²⁰ Spectra were simulated using a program developed by D. B. Bailey in these laboratories and is used in conjunction with a CALCOMP plotter.⁸ The free induction decay (FID) is generated using the following algorithm:

$$F_1 = \sum_{N=1}^{\text{NPKS}} A_N \cos(2\pi\nu_N t) \exp(-t/T_{2N})$$

where F_1 is the amplitude of the FID at time t , NPKS is the number of resonance lines, ν_N , A_N , and T_{2N} are the resonant frequency, initial amplitude, and decay constant, respectively. The program includes routines to produce noise, simulate dynamic range, field inhomogeneity, and zero filling so that the data message is as similar as feasible to results obtained from the NMR spectrometer.

Results

$\text{B}(\text{OCH}_3)_3$. The spin-lattice and transverse relaxation times were determined for both the ^{10}B and ^{11}B nuclei of an isotopically normal sample of $\text{B}(\text{OCH}_3)_3$. For the ^{10}B nucleus at 0

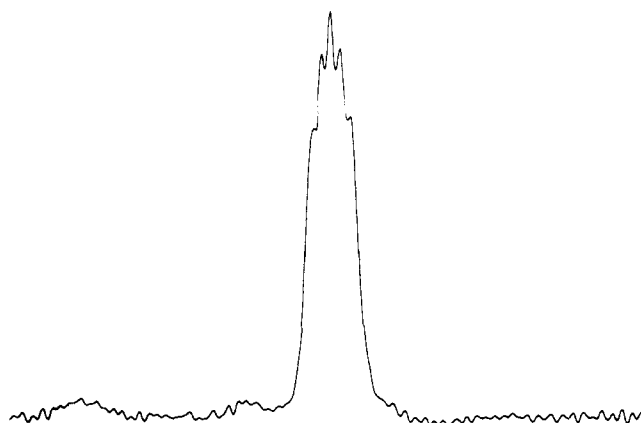


Figure 2. The line-narrowed ^{10}B NMR spectrum of the B(1,3) resonance of $^{11}\text{B}_4\text{H}_{10}$ obtained at 10.7 MHz and 0 °C. The unexpected multiplicity of lines is probably the result of partial thermal collapse of the multiplet.

°C, $T_1 = 12.4$ and $T_2 = 12.3$ ms. For the ^{11}B nucleus at 35 °C, $T_1 = 12.9$ and $T_2 = 13.0$ ms.

B_2H_6 , B_4H_{10} . The spin-lattice relaxation time (T_1) was measured for a 96% ^{11}B enriched sample of B_2H_6 . At -20 °C, the T_1 was 24.2 ms, which defines a half-height line width of 13.2 Hz. At -20 °C, the experimental half-height line width observed with complete proton decoupling is 14.0 Hz. An error of $\pm 5\%$ in the accuracy of the T_1 measurement implies a range of 12.5–13.9 Hz for the calculated $\Delta\nu_{1/2}$. The close agreement between calculated and observed values lends support to the assumption that $T_1 = T_2$ and also indicates little additional line broadening due to inhomogeneity in the magnetic field. Additionally, the simplicity of this system makes it an ideal case to check the ability of the FIDMKR program to reproduce the experimental line shape (Figure 1).

The ^{11}B spin-lattice relaxation times, measured for an isotopically ^{11}B enriched sample of B_4H_{10} , are 62.6 ms for the B(1,3)²¹ resonance and 13.1 ms for the B(2,4) resonance at -20 °C. These values define half-height line widths of 5.1 and 24.4 Hz for the B(1,3) and B(2,4) resonances, respectively. The observed half-height line widths at -20 °C are 9.0 Hz for the B(1,3) resonance and 29.0 Hz for the B(2,4) resonance. The difference between observed and calculated values is considerably greater than expected in terms of accuracy in determination of the T_1 's and suggests that additional line broadening due to boron-boron coupling is present. Using the experimentally determined T_1 's, the value of $J_{\text{B}_1\text{B}_2}$ was varied in the FIDMKR program to achieve a simultaneous best fit of both experimental half-height line widths. The value of the coupling constant determined in this fashion is 1.0 Hz and represents an upper limit, since inhomogeneity in H_0 can also cause additional line broadening.

In an attempt to directly measure the magnitude of $J_{\text{B}_1\text{B}_2}$ in B_4H_{10} , the ^{10}B spectrum of a ^{11}B enriched sample was obtained (Figure 2). The observed multiplicity of lines is not what one might expect for a spin 3 nucleus coupled to a single spin $3/2$ nucleus and is currently under further investigation. However, it is apparent from the observed half-height line width that the magnitude of the ^{11}B - ^{11}B coupling constant through the B(1)-B(3) bond in B_4H_{10} is no greater than 25 Hz.

The ^{10}B spin-lattice relaxation times measured are B(1,3), 136.3 and B(2,4), 29.1 ms. The analogous T_2 's are B(1,3), 130.0 and B(2,4), 28.7 ms, and within experimental error are equal to the measured T_1 's.

$\text{B}_3\text{H}_7\cdot\text{CO}$. The experimentally determined T_1 's and calculated half-height line widths at -35 °C for the molecule are 18.9 ms (calcd $\Delta\nu_{1/2} = 16.8$ Hz) for the B(1) resonance and 10.7 ms (calcd $\Delta\nu_{1/2} = 29.7$ Hz) for the B(2,3) resonance. The

Table I.

Molecule ^a	T_1 , ms	T_2 , ms	τ^b	Temp, °C	Calcd $\Delta\nu_{1/2}$, Hz ^c	$\Delta(\text{expt} - \text{calcd})$, Hz ^d	$J_{^{11}\text{B}^{11}\text{B}}$, Hz
$\text{B}(\text{OCH}_3)_3(^{11}\text{B})$	12.9	13.0		35.0			0
$\text{B}(\text{OCH}_3)_3(^{10}\text{B})$	12.4	12.3		0.0			0
$^{11}\text{B}_2\text{H}_6$	24.2		20	-20.0	13.2	0.8	0
$^{11}\text{B}_4\text{H}_{10}(^{11}\text{B})$							
B(1,3)	62.6		27	-20.0	5.1	3.9	$J_{\text{B}_1\text{B}_2} = 1.0$
B(2,4)	13.1		16	-20.0	24.4	4.6	$J_{\text{B}_1\text{B}_3} \leq 25$
$^{11}\text{B}_4\text{H}_{10}(^{10}\text{B})$							
B(1,3)	136.3	130.0	10	0.0			
B(2,4)	29.1	28.7	10	0.0			
$\text{B}_3\text{H}_7\text{-CO}$							
B(1)	18.9		18	-35.0	16.8	33.2	$J_{\text{B}_1\text{B}_2} = 11$
B(2,3)	10.7		20	-35.0	29.7	20.3	
B_5H_9							
Base	63.6		19	60.0	5.0		$J_{\text{B}_1\text{B}_2} = 19.4$
B_5H_{11}							
B(1)	54.9		10	-20.0	5.7	59.3	$J_{\text{B}_1\text{B}_3} = 17$
B(2,5)	7.5		10	-20.0	42.0	5.0	
B(3,4)	20.7		16	-20.0	15.2	45.8	

^a Both ^{10}B and ^{11}B nuclei were examined for $\text{B}(\text{OCH}_3)_3$ and $^{11}\text{B}_4\text{H}_{10}$. The nucleus to which the data pertains is enclosed in parentheses. ^b Number of data points used in least-squares analysis. ^c Calculated as: $\Delta\nu_{1/2} = 1/\pi T_1$. ^d Difference between observed and calculated half-height line widths.

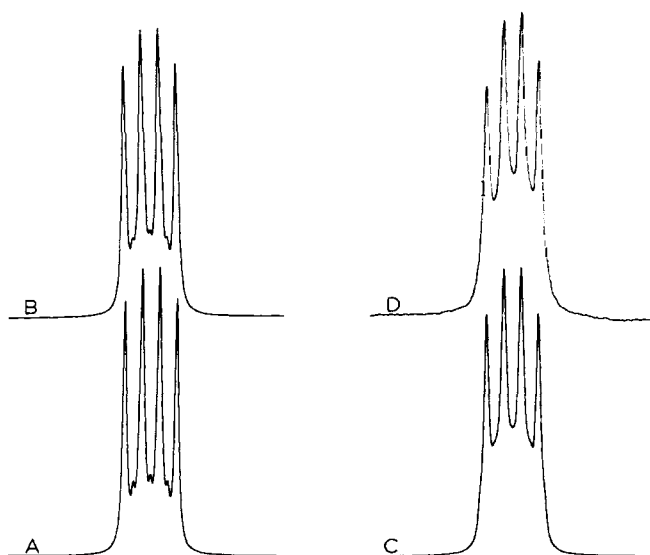


Figure 3. (A) Calculated ^{11}B NMR spectrum of the basal resonance of B_5H_9 , utilizing the 63.6 ms T_1 measured at 60 °C, $J_{\text{B}_1\text{B}_2} = 19.4$ Hz, and assuming a 4.0 $^{11}\text{B}/^{10}\text{B}$ isotopic abundance ratio; (B) same as A, but including $J_{\text{B}_1\text{B}_2\text{B}_3} = 1.0$ Hz; (C) best fit to experimental curve, utilizing the measured T_1 , $J_{\text{B}_1\text{B}_2} = 19.4$ Hz, $J_{\text{B}_1\text{B}_3} = 0.0$ Hz, and $J_{\text{B}_1\text{B}_4} = 5.0$ Hz; (D) experimental curve at 60 °C.

observed half-height line width is 50.0 Hz for both resonances. Line-narrowing techniques failed to resolve any boron-boron coupling; therefore, the magnitude of the coupling constant was determined by line fitting using the FIDMKR NMR simulation program. The B(2,3) resonance was simulated by varying the value of J_{BB} and using the measured T_1 . A coupling constant of 11 Hz produced a best fit. This coupling constant together with the 18.9 ms T_1 then led to a simulated line shape of the B(1) resonance, also in good agreement with the observed spectrum.

$\text{B}_4\text{H}_8\cdot\text{L}$. We have recently reported the value of $J_{\text{B}_1\text{B}_3}$ in $\text{B}_4\text{H}_8\cdot\text{L}$ to be 24 Hz.¹ We have now measured this coupling constant for the related molecules $\text{B}_4\text{H}_8\cdot\text{L}$ ($\text{L} = \text{PF}_2\text{N}(\text{CH}_3)_2$, PF_3 , PF_2H) and have found the value to be 24 ± 1 Hz in all cases. The magnitude of the coupling constant was directly measured using line-narrowing techniques.

B_5H_9 . The value of the apex base coupling constant in B_5H_9 has been previously reported to be 19.4 Hz.⁴ Utilization of this coupling constant and the 63.6 ms T_1 measured for the basal resonance at 60 °C yielded the spectrum shown in Figure 3A. The spectrum was simulated again assuming magnetic non-equivalence in the base caused by the presence of the ^{10}B isotope, thereby introducing boron-boron coupling within the base. A coupling constant of 1.0 Hz between adjacent borons (derived for boron-boron coupling through a BHB bridge bond in B_4H_{10}) yields the spectrum shown in Figure 3B. Numerous combinations of boron-boron coupling constants²⁸ between adjacent (B(2)-B(3)) and antipodal (B(2)-B(4)) borons within the base were computed. Figure 3C ($J_{\text{B}_2\text{B}_3} = 5.0$, $J_{\text{B}_2\text{B}_4} = 0.0$ Hz) represents the best fit to the observed spectrum, Figure 3D.

B_5H_{11} . The T_1 's and calculated half-height line widths at -20 °C for this molecule are: B(1), $T_1 = 54.9$ (calcd $\Delta\nu_{1/2} = 5.7$ Hz); B(2,5), $T_1 = 7.5$ (calcd $\Delta\nu_{1/2} = 42$ Hz); B(3,4), $T_1 = 20.7$ ms (calcd $\Delta\nu_{1/2} = 15.2$ Hz). The differences in observed and calculated half-height line widths are: B(1), 59.3; B(2,5), 5.0; B(3,4), 45.8 Hz. These data indicates strong coupling between the apical boron and B(3,4). Indeed, this coupling can be resolved using line-narrowing techniques and we have determined a value of 17 Hz, in agreement with previous studies.⁷

$\text{B}_{10}\text{H}_{14}$. The magnitude of $J_{\text{B}_2\text{B}_6}$ was measured directly by line narrowing of the proton-decoupled ^{11}B NMR spectrum in CS_2 (~1 M) at ambient temperature. The coupling constant so derived has a value of 18.7 Hz.

Discussion

Previous studies by Allerhand et al.⁹ have shown that the dominant T_1 relaxation mechanism of the ^{10}B and ^{11}B nuclei is quadrupolar. There is, however, an additional relaxation mechanism which may be effective for transverse (T_2) relaxation of these nuclei. Scalar relaxation can contribute to the T_2 of any coupled spin system; therefore, its effectiveness must be evaluated before the assumption that $T_1 = T_2$ is established for the boron hydrides.

For a molecule in which boron-boron coupling is absent, scalar relaxation does not contribute to the T_2 . We have measured both T_1 and T_2 of $^{10}\text{B}(\text{OCH}_3)_3$ and $^{11}\text{B}(\text{OCH}_3)_3$ and within experimental error $T_1 = T_2$ for both isotopes: at 0

°C for $^{10}\text{B}(\text{OCH}_3)_3$, $T_1 = 12.4$ and $T_2 = 12.3$ ms; for $^{11}\text{B}(\text{OCH}_3)_3$ at 35 °C, $T_1 = 12.9$ and $T_2 = 13.0$ ms. Simple exponential decays are observed in both cases. Nonexponential relaxation²² is expected for a nucleus with $I > 1$ only if the extreme narrowing condition is not valid.

The T_1 and T_2 relaxation rates of the ^{10}B nuclei in an ^{11}B enriched sample of B_4H_{10} were investigated to ascertain the importance of scalar relaxation in a molecule where heteronuclear ^{10}B - ^{11}B coupling is present. Complications in the measurement of T_2 arising from homonuclear coupling are avoided due to the isotopic dilution of the ^{10}B nuclei. Tetraborane(10), a priori, represents a case where T_2 scalar relaxation may be significant relative to T_2 quadrupolar relaxation. From the equation

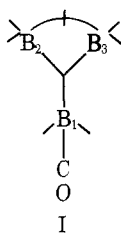
$$1/T_2^{\text{SC}} = \frac{A^2}{3} S(S+1) \left[\tau_S + \frac{\tau_S}{1 + (W_I - W_S)^2 \tau_S^2} \right] \quad (1)$$

one might expect a significant contribution from scalar relaxation when A , the scalar coupling in rad/s, is large and/or when S , the nuclear spin number, is large. For B_4H_{10} , Bal-deschiwiler et al.²³ have predicted $J_{\text{B}_1\text{B}_3}$ to be 50 Hz. This predicted coupling constant is clearly larger than any boron-boron coupling constant reported to date. The results presented above clearly indicate that for B_4H_{10} and other boron hydrides in which J_{BB} is less than or equal to $J_{\text{B}_1\text{B}_3}$ of B_4H_{10} , the contribution of heteronuclear scalar mechanisms to ^{10}B transverse relaxation is negligible. Presumably, this argument can be extended to ^{11}B , vide supra eq 1. This conclusion provides the basis for the use of the FIDMKR program for extracting boron-boron coupling constants from a knowledge of line shape and *spin-lattice* relaxation times only.

Our intention at the outset of this investigation was to measure boron-boron coupling constants for bonding environments not previously studied. We have found that the magnitude of J_{BB} varies considerably depending on the type of bond between the coupled atoms. In terms of the localized MO calculations of Lipscomb,²⁴ we have found that in situations where we observe a large coupling constant, electron density difference maps also indicate a buildup of electron density between the coupled centers. While intuitively it seems reasonable to expect a larger coupling constant when there is greater electron density between the coupled atoms, this has not been rigorously shown theoretically.

For two boron atoms bonded through a three-center, two-electron BHB bridge bond, the electron density along the internuclear boron-boron axis is very low.^{25,26} The observed boron-boron coupling constant through a BHB bridge bond is also observed to be small. Previous estimates of J_{BB} in B_2H_6 ⁵ put an upper limit of 1.1 Hz on that coupling constant. In this study, we have determined an upper limit of 1.0 Hz for $J_{\text{B}_1\text{B}_2}$ in B_4H_{10} .

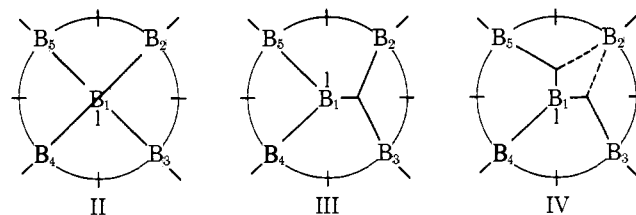
Although there has been no theoretical treatment of the bonding in $\text{B}_3\text{H}_7\text{-CO}$, the structure has been determined by Schaeffer et al.,¹³ which corresponds to a bonding situation in "styx" notation of 1104 as shown below. This molecule rep-



resents a rather simple spin system for which a boron-boron coupling constant ($J_{\text{B}_1\text{B}_2}$) through a closed three-center, two-electron BBB bond could be determined. This coupling constant was determined to be 11 Hz, considerably greater than

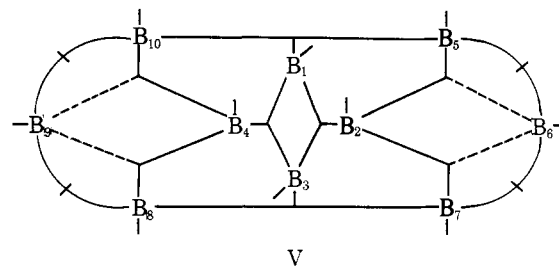
J_{BB} through a BHB bridge bond. Since an electron density difference map is not available for $\text{B}_3\text{H}_7\text{-CO}$, it is desirable to look at another molecule which also contains a closed three-center, two-electron bond and for which these maps are available, such as $\text{B}_{10}\text{H}_{14}$.²⁷ Inspection of an electron density difference map in the B(1)B(2)B(3) plane of $\text{B}_{10}\text{H}_{14}$, which approximates a symmetrical, closed three-center, two-electron BBB bond, indicates some buildup of electron density along the internuclear axes.

The boron framework bonding in B_5H_9 is more difficult to define.²⁴ A variety of resonance structures can be envisioned.



Each of the structures presented is, however, one of several equivalent resonance hybrids. What can be seen in each static structure is that the bonding between the apex and basal borons is a combination of a three-center, two-electron and two-center, two-electron BB bond. The electron density between any basal boron and the apex should be intermediate between these two extremes. The apex to basal boron-boron coupling constant is 19.4 Hz⁴ and is considerably larger than the 11 Hz coupling constant derived from our study of $\text{B}_3\text{H}_7\text{-CO}$.

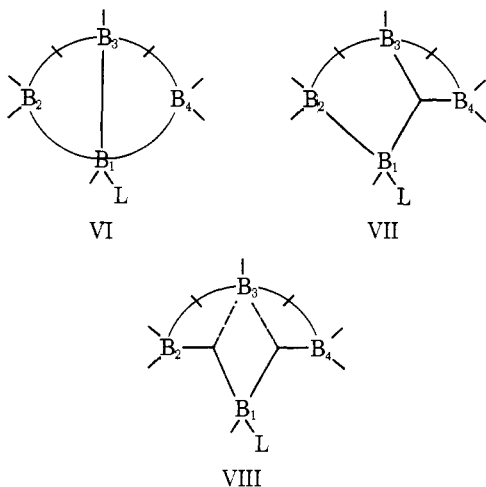
The resonance structure employing the fractional three-center bond (IV) strongly resembles the bonding between B(2)B(5)B(6) and B(7) of $\text{B}_{10}\text{H}_{14}$. Again, alternative valence



structures can be drawn that give some two-center, two-electron bond character to the B(2)-B(6) bond. The similarity of the B(2)-B(6) bond in $\text{B}_{10}\text{H}_{14}$ to the B(1)-B(2) bond (IV) in B_5H_9 is also reflected in the similarity of the coupling constants; $J_{\text{B}_1\text{B}_2}(\text{B}_5\text{H}_9) = 19.4$ and $J_{\text{B}_2\text{B}_6}(\text{B}_{10}\text{H}_{14}) = 18.7$ Hz.

The basal boron resonance of B_5H_9 was further investigated to ascertain the degree of boron-boron coupling within the base. Incorporation of the measured T_1 of the basal resonance and the 19.4 Hz apex to base coupling constant in the FIDMKR simulation program produced a spectrum too rich in detail (Figure 3A). Although the 5.0 Hz B(2)-B(4) coupling which produces the best fit to the experimental line shape in our study may not be a unique solution, it is clear that inclusion of some boron-boron coupling within the base of B_5H_9 is necessary to explain the experimentally observed pattern.

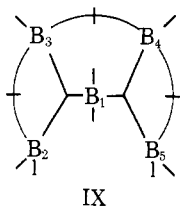
We investigated the series of molecules $\text{B}_4\text{H}_8\text{-L}$ ($\text{L} = \text{CO}$, PF_3 , HPF_2 , $(\text{CH}_3)_2\text{NPF}_2$), since the chemical and magnetic nonequivalence of B(1) and B(3) allows direct observation of $J_{\text{B}_1\text{B}_3}$. In the classical presentation of the bonding (VI),²⁹ these molecules contain a two-center, two-electron B(1)-B(3) bond. This description of the bonding necessitates, however, an open three-center, two-electron B(2)B(1)B(4) bond. More recent treatments of bonding in neutral boron hydrides²⁴ exclude the use of open three-center, two-electron BBB bonds. Alternative resonance structures that may be drawn are VII and VIII. We have found that $J_{\text{B}_1\text{B}_3}$ for all $\text{B}_4\text{H}_8\text{-L}$ molecules studied is 24



± 1 Hz. This is the largest value of J_{BB} found in this study. Several conclusions can be drawn. Structure VII seems unfavorable, since it implies a large B(1)-B(2) coupling which was not found. Structure VI is considered unfavorable, since it requires an open three-center, two-electron BBB bond. Thus structure VIII would seem to be the best single representation of the bonding in the molecules $B_4H_8 \cdot L$. There is, however, an alternative conclusion equally consistent with our NMR data. The molecules $B_4H_8 \cdot L$ are isoelectronic with $B_4H_9^-$ and therefore represent a case where the open three-center, two-electron bond BBB has not been excluded. Structure VI, which contains this open three-center, two-electron BBB bond, also contains a two-center, two-electron B(1)-B(3) bond. The large B(1)-B(3) coupling constants (24 Hz) measured for the molecules $B_4H_8 \cdot L$ is comparable to the upper limit of 25 Hz estimated for $J_{B_1B_3}$ (see Results, B_4H_{10}) in B_4H_{10} , which has been shown to contain a localized two-center, two-electron B(1)-B(3) bond. A reasonable conclusion is that the similarity of $J_{B_1B_3}$ observed for $B_4H_8 \cdot L$ and B_4H_{10} reflects analogous bonding between B(1) and B(3) in both systems. Thus structure VI remains a viable representation of the bonding in the molecules $B_4H_8 \cdot L$. This apparent ambiguity will require further experimental and theoretical work to resolve the question of bonding in these molecules.

The apparent insensitivity of $J_{B_1B_3}$ to the variation of the substituent L contrasts sharply with a previous study of substituent effects of $J_{B_1B_2}$ for apically substituted B_5H_9 derivatives.³⁰ This may be a manifestation of the similarity of the substituents used in this study.

Perhaps the best correlation between J_{BB} and the electron density difference maps is found in B_5H_{11} . Lipscomb et al. have found that the bonding in B_5H_{11} is best represented by structure IX.³¹ Their calculations indicate an asymmetry in the



B(1)B(2)B(3) closed three-center, two-electron bond with much greater electron density between B(1) and B(3) than between B(1) and B(2). We observe a large coupling of 17 Hz between B(1) and B(3). The B(1)-B(2) coupling constant,

while not explicitly determined in this study, is clearly less than 2 Hz from measured line widths.

In summary, we have shown that from a knowledge of line shape and spin-lattice relaxation times, unresolved boron-boron coupling constants can be estimated. Utilization of T_1 's for the line-shape analysis is justified, since it is rigorously shown that T_1 is equal to T_2 for the molecules studied. For each of the common bonding environments, a substantially different boron-boron coupling constant was observed. The magnitude of J_{BB} qualitatively correlates with increased electron density along the internuclear boron-boron axis, as illustrated by localized MO electron density difference maps derived by other investigators.²⁴

Acknowledgment. The authors gratefully acknowledge Mr. D. B. Bailey's valuable contribution to the spectral simulation portion of this study. The authors also gratefully acknowledge the financial support of this work by the National Science Foundation through Grant GP-42454X.

References and Notes

- (1) Part 5: E. J. Stampf, A. R. Garber, J. D. Odom, and P. D. Ellis, *Inorg. Chem.*, **14**, 2446 (1975).
- (2) Taken in part from the thesis of E. J. Stampf, submitted to the Graduate School of the University of South Carolina in partial fulfillment of the requirements for the Ph.D. degree, Aug 1976.
- (3) Unless otherwise stated, J_{BB} refers to a ^{11}B - ^{11}B spin coupling constant.
- (4) J. D. Odom, P. D. Ellis, and H. C. Walsh, *J. Am. Chem. Soc.*, **93**, 3529 (1971).
- (5) J. D. Odom, P. D. Ellis, D. W. Lowman, and M. H. Gross, *Inorg. Chem.*, **12**, 95 (1973).
- (6) R. R. Ernst, *Adv. Magn. Reson.*, **2**, 1 (1966).
- (7) A. O. Clouse, D. C. Moody, R. R. Rietz, T. Roseberry, and R. Schaeffer, *J. Am. Chem. Soc.*, **95**, 2496 (1973).
- (8) D. Bailey and P. D. Ellis, *J. Chem. Educ.*, submitted for publication.
- (9) A. Allerhand, J. D. Odom, and R. E. Moll, *J. Chem. Phys.*, **50**, 5037 (1969).
- (10) A. Abragam, "The Principles of Nuclear Magnetism", Oxford University Press, London, 1961.
- (11) D. F. Shriver, "The Manipulation of Air-Sensitive Compounds", McGraw-Hill, New York, N.Y., 1969.
- (12) I. Shapiro, H. G. Weiss, M. Schmick, S. Skolnich, and G. B. L. Smith, *J. Am. Chem. Soc.*, **74**, 901 (1952).
- (13) J. D. Giore, J. W. Rathke, and R. Schaeffer, *Inorg. Chem.*, **12**, 2175 (1973).
- (14) J. R. Spielman and A. B. Burg, *Inorg. Chem.*, **2**, 1139 (1963).
- (15) R. W. Rudolph and H. W. Schiller, *J. Am. Chem. Soc.*, **90**, 3581 (1968).
- (16) R. Schmutzler, *Inorg. Chem.*, **3**, 415 (1964).
- (17) G. Ter Haar, M. A. Fleming, and R. W. Parry, *J. Am. Chem. Soc.*, **84**, 1767 (1962).
- (18) L. F. Centofanti, G. Kodama, and R. W. Parry, *Inorg. Chem.*, **8**, 2072 (1969).
- (19) S. Meiboom and D. Gill, *Rev. Sci. Instrum.*, **29**, 688 (1958).
- (20) Details of the implementation of this procedure on a Varian XL-100-15 to appear elsewhere, R. A. Byrd, A. R. Garber, and P. D. Ellis, manuscript in preparation.
- (21) The numbering system is that recommended for boron compounds by the Council of the American Chemical Society, *Inorg. Chem.*, **7**, 1945 (1968).
- (22) P. S. Hubbard, *J. Chem. Phys.*, **53**, 985 (1970).
- (23) R. C. Hopkins, J. D. Baldeschwieler, R. Schaeffer, F. N. Tebbe, and A. Norman, *J. Chem. Phys.*, **43**, 975 (1965).
- (24) W. N. Lipscomb, *Acc. Chem. Res.*, **6**, 257 (1973), and references cited therein.
- (25) E. Switkes, R. M. Stevens, and W. N. Lipscomb, *J. Chem. Phys.*, **51**, 2085 (1969).
- (26) E. Switkes, I. R. Epstein, J. A. Tossell, R. M. Stevens, and W. N. Lipscomb, *J. Am. Chem. Soc.*, **92**, 3837 (1970).
- (27) E. A. Laws, R. M. Stevens, and W. N. Lipscomb, *J. Am. Chem. Soc.*, **94**, 4467 (1972).
- (28) For studies of the boron-boron coupling within the base of isotopically normal B_5H_9 , a special patch was added to the FIDMKR program which allowed calculation of all possible transition frequencies and amplitudes for any given combination of $J_{B_1B_2}$, $J_{B_2B_3}$, and $J_{B_2B_4}$.
- (29) W. N. Lipscomb, "Boron Hydrides", W. A. Benjamin, New York, N.Y., 1963.
- (30) D. W. Lowman, P. D. Ellis, and J. D. Odom, *Inorg. Chem.*, **12**, 681 (1973).
- (31) E. Switkes, W. N. Lipscomb, and M. D. Newton, *J. Am. Chem. Soc.*, **92**, 3847 (1970).